Universities Council on Water Resources
Journal of Contemporary Water Research & Education
Issue 171, Pages 93-110, December 2020

Integrated Hydrologic and Hydraulic Analysis of Torrential Flood Hazard in Arequipa, Peru

*Katy E. Mazer[1], Abigail A. Tomasek[2], Fariborz Daneshvar[2], Laura C. Bowling[1], Jane R. Frankenberger[2], Sara K. McMillan[2], Hector M. Novoa[3], and Carlos Zeballos-Velarde[4]

*[1]Department of Agronomy, Purdue University, West Lafayette, IN, USA; [2]Department of Agricultural and Biological Engineering, Purdue University, West Lafayette, IN, USA; [3]Faculty of Civil Engineering, Universidad Nacional de San Agustín de Arequipa, Arequipa, Peru; [4]Faculty of Architecture and Urbanism, Universidad Nacional de San Agustín de Arequipa, Arequipa, Peru; *Corresponding Author*

Abstract: Seated at the foot of the Misti volcano in an area prone to intense seasonal rains and earthquakes, the city of Arequipa is highly vulnerable to natural disasters. During the rainy season, intense storms create large volumes of runoff that rush through the city's ephemeral streams, known locally as *torrenteras*. Episodic flows in these *torrenteras* have caused flooding, damage to bridges, homes, and other infrastructure, and caused many deaths. In recent years, while unprecedented rain events have caused extreme disasters, the city's population has continued to expand into these channels by creating informal or illegal settlements. Currently, detailed hazard maps of flood-prone areas surrounding the *torrenteras* are not available to stakeholders in Arequipa. In this study, hydrologic and hydraulic models were combined to assess flash flood hazards, including inundation, velocity hazards, and slope instability hazards. Hydrologic models were created using satellite precipitation data and terrain-sensitive, gridded climate maps to characterize flow within six *torrenteras* in Arequipa. These flows were used in conjunction with elevation data and data collected in the field using an online mobile application system to develop a hydraulic model of these flood events. Hydraulic model outputs were used to determine flood hazards related to inundation, velocity affecting human stability, and slope instability in case study areas of the *torrenteras*. We then discuss how this information can be used by disaster risk management groups, water authorities, planners and municipalities, and community groups.

Keywords: *torrenteras, hydrologic modeling, hydraulic modeling, flash floods, inundation, velocity, slope instability, hazard maps*

Arequipa, the second largest city in Peru, is located at the foot of El Misti volcano. Rain that falls on the eastern side of the mountain drains through the city in ephemeral stream channels as destructive flash floods. Although annual precipitation within the city ranges from 100 - 150 mm on average, torrential flows occur during the rainy season through the channels that extend from their source on the mountain where rainfall is higher (Figure 1). These channels or ravines are known locally as "*torrenteras,*" signifying not only their channel shape but also the torrential flows that occur in these channels after intense rainfall. Six major *torrenteras* flow through the lower elevations of the mountainside, where residential development is increasing, and into the core of the city. Local names of each *torrentera* will be used throughout this paper (Figure 1), though common names may change further downstream.

Flash floods in the *torrenteras* of Arequipa have had devastating effects on the city's population throughout its history. Nine events that caused severe damage occurring from 1961 to 2011 were summarized by Martelli (2011) from government and other records. An exceptional flood occurred on February 8, 2013 due to a rainfall of 123 mm in three hours (Cacya et al. 2013), causing five deaths and adversely affecting thousands more people (SINPAD 2013). As the city has continued to grow, some structures have been built close to or even within the *torrenteras*, adding to the devastation that floods can cause (Thouret et al. 2013).

In this paper, we define hazards as geophysical features or processes that can cause drastic changes to a landscape. Hazards become risks when they affect people or infrastructure and are amplified when those affected are more vulnerable either due to socioeconomic, health, or simply proximity to the hazard itself. Flash floods are among the highest risk weather-related phenomena in cities around the world, resulting in more than 15,600 fatalities in China from 2000 to 2015 (He et al. 2018), and 278 deaths in the United States during an eight-year period ending in 2015 (Gourley et al. 2017), for example. In addition to the potential for inundation, floodwaters present other dangers, including water velocity hazards that can endanger humans (Jonkman and Penning-Rowsell 2008) and vehicles (Martinez-Gomariz et al. 2016), and slope instability hazards that threaten surrounding infrastructure due to bank failure (Magilligan et al. 2015). Flood hazards are projected to increase in the future in many regions from increasing precipitation intensity and changes in land cover affected by climate change and population growth, potentially leading to heavy human and economic losses in these communities (Muller 2007). It is generally not possible to eradicate these precipitation-driven flood hazards; instead, the risk management strategy usually focuses on reducing vulnerability by informing the public and enacting policies that discourage encroachment into the channels where these hazards are likely to occur. In Arequipa, current regulations limiting construction are based solely on the distance from the edge of the *torrenteras*, but do not account for the varying characteristics of flows and flood hazard (Republica de Perú 2016).

Although flood hazards from the *torrenteras* have been studied in the past, these have been based on topography and geomorphology of the landscape because no discharge monitoring data are available. Thouret et al. (2013) studied flash floods and lahars (volcanic mudflows) in the Rio Chili, the main river that runs through the city of Arequipa, and two of the *torrenteras*, which they

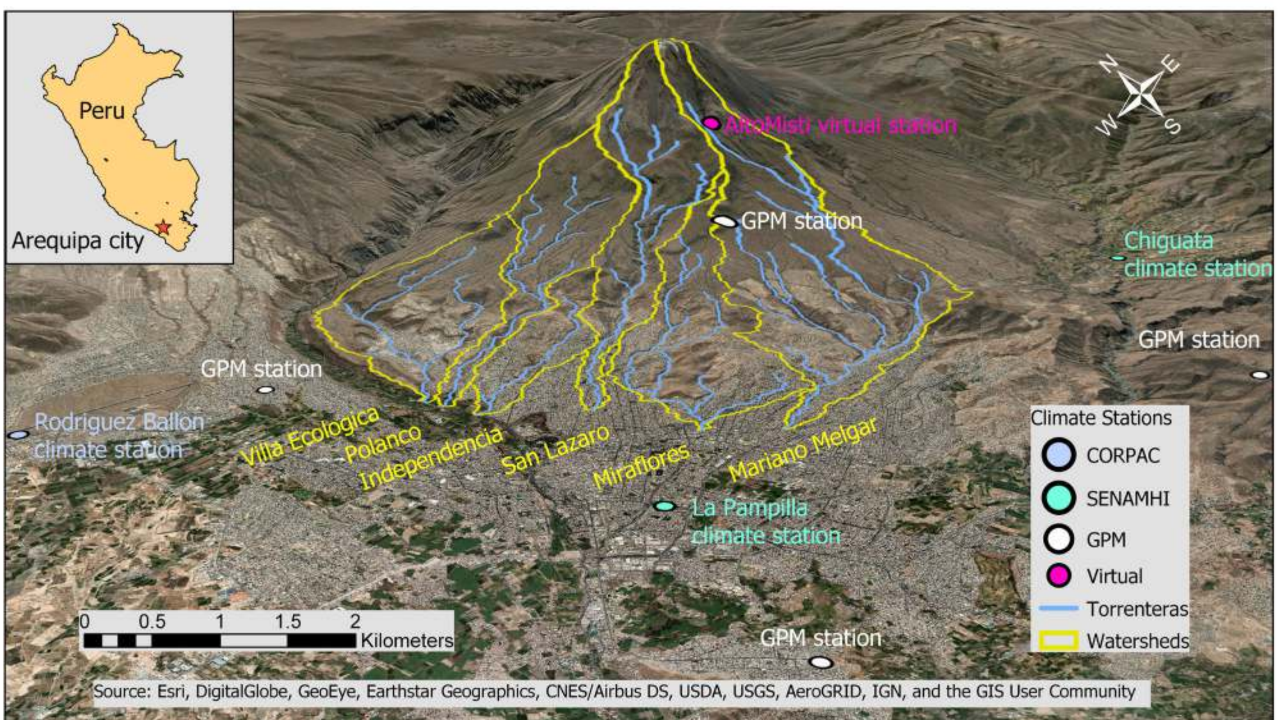

Figure 1. *Torrentera* flow paths from El Misti through the city of Arequipa and climate stations used for analysis.

call *quebradas* (San Lázaro and Mariano Melgar in this study, called Huarangal in their study) to create hazard maps. However, the morphology-based analysis from this study does not allow for examining changes over time, which instead requires hydrologic and hydraulic modeling based on observed and projected changes in precipitation.

Developing flood hazard maps is generally a two-step process, requiring first a hydrologic analysis to determine the magnitude of low-probability (i.e., 100-year) storm discharge, and then using a hydraulic model to estimate flow depth for the discharge of concern. In watersheds such as the *torrenteras* for which no discharge data exist, hydrologic models that compute discharge on the basis of rainfall and watershed characteristics such as land cover, soil, and slope, are used to estimate flow. Hydraulic models can use the modeled discharge together with high-resolution channel elevation data to calculate flood depth and predict hazards. However, data scarcity often limits the application of these powerful tools. For this project, high-resolution elevation data captured by an unmanned aircraft system (drone) were available for a section of the six *torrenteras*, providing a unique opportunity for hydraulic modeling.

Providing useful data to decision-makers is a primary purpose of a modeling study such as this. In Arequipa, four types of stakeholders would benefit from this type of flood modeling. The types of activities for which they are responsible are as follows:

- **Disaster risk management**: Peru's Law No. 29664 created the National Disaster Risk Management System (SINAGERD) as well as two institutions related to risk management: the National Center for Estimation, Prevention and Reduction of Disaster Risk (CENEPRED), responsible for disaster prevention and post-disaster reconstruction; and the National Civil Defense Institute (INDECI), responsible for emergency response activities.
- **Water authority**: Water courses are regulated in Peru by the National Water Authority (ANA), and its local branch the Local Water Authority (ALA), which is responsible for determining the flood boundaries and buffer zones for limited development.
- **Municipalities and planners:** The Urban Development Department, Office of Disaster Risk Management and Civil Defense, and the Office of the Environment prepare and respond to disaster events, while the Inspections Office works to limit new informal settlements in the area of the *torrenteras*. In the event of a major disaster, the municipality coordinates with the National Government and the Ministry of Housing and Construction on reconstruction.
- **Communities**: People who live in the affected communities are grouped into brigades and organized to prepare for disasters through citizen security committees. Zeballos-Velarde et al. (2019) found that community groups identify areas in Arequipa with critical environmental problems, but their perception of the spatial extents of flood impacts is often distorted.

These stakeholders are interested in acting effectively to reduce risk, but do not have access to information needed to make decisions. A detailed study would aid development planning by defining areas that are at risk and areas where complementary activities could be carried out to transform specific locations within the *torrenteras* from marginal lands into recreational spaces.

The goal of this study is to provide information on flood hazards in the six *torrenteras* of Arequipa that is useful to these stakeholders. The objectives of this study were to 1) analyze precipitation patterns and flow magnitude and how they have changed over time, 2) identify locations and extent of flood-related hazards, including inundation, velocity, and slope instability, and 3) discuss relevance for multiple stakeholder groups. Analysis of precipitation records and sub-daily estimates from satellite data provided input for the hydrologic model, resulting in long-term discharge estimates for each *torrentera*. The discharge estimates were used as inputs for hydraulic models built for each *torrentera* to estimate flood depths and velocities. Hazard classifications were developed, and examples are shown to demonstrate how stakeholders can use this information.

Methods

Precipitation

Daily precipitation data for two nearby stations were obtained from the National Meteorology and Hydrology Service of Peru (SENAMHI 2019, see Figure 1). SENAMHI climate stations, La Pampilla and Chiguata, were closest to the *torrenteras* and ranged from 2 to 4 km away. A third station, the Rodríguez Ballón airport in the city of Arequipa, is not available in the SENAMHI dataset, but is instead administered by the Peruvian Corporation of Airports and Commercial Aviation (CORPAC). A virtual weather station (hereafter called AltoMisti) was added to provide information of precipitation contributing to the *torrentera* watersheds in the study area (Location: -16.32° W, -71.42° S; Elevation: 4200 m), based on gridded, terrain-corrected climate maps developed from SENAMHI station data (Moraes et al. 2019).

This analysis required precipitation data at a time scale of hourly or less, because the time of concentration in the *torrenteras* is less than one hour. In recent years, the daily network has been supplemented with sub-daily automated gauges, but most of these gauges currently have a record length of less than five years. Therefore, we disaggregated observed daily precipitation to sub-daily in order to simulate flood response. The GPM_3IMERGHH_v06 (hereafter referred to as GPM) satellite precipitation product, available globally at 30-minute temporal resolution and 0.1 degree spatial resolution, was downloaded for grid cells corresponding to the three SENHAMI precipitation gauges and one synthetic gauge, and adjusted from Coordinated Universal Time (UTC) to Peruvian Standard Time (UTC-5) (Huffman et al. 2019). The data period of overlap with the SENHAMI stations was 6/1/2000 - 12/31/2017. Quality control screening for the GPM data included setting precipitation to zero for all 30-minute intervals in the days for which the corresponding station precipitation was zero. Additionally, if the accumulated daily intensity in the GPM data exceeded the maximum intensity observed at the corresponding daily station for the 17 years of overlap, all 30-minute values on that date were rescaled. The quality controlled GPM data were bias-corrected with respect to the station observations using linear scaling with the ratio of accumulated station precipitation to GPM precipitation (Teutschbein and Seibert 2012).

A 30-minute precipitation time series was created for the period February 1965 - March 2020 by disaggregating the station observations using a point, event-based, rectangular pulse model (Rodriguez-Iturbe et al. 1987). However, rather than simulating storm interarrivals as a Poisson process, the observed daily sequence was used, similar to Bowling et al. (2003). Each daily occurrence is associated with rainfall events of random duration and intensity. The bias-corrected GPM estimations were used to identify the empirical cumulative distribution functions (CDF) of the number of events per day, the event start time, and the event duration. Three different duration CDFs were generated for event depths of < 5 mm, 5-10 mm, and > 10 mm, since event durations tend to be shorter for lower precipitation totals. For each day with observed daily precipitation, the event CDF was sampled randomly to generate the number of events per day. The corresponding start time and duration distributions were then sampled to determine which hours of the day should receive precipitation. Within the identified hours, the observed daily precipitation depth was distributed, using a gaussian window to create a higher intensity peak in the center of the event.

Intensity-frequency diagrams were used to evaluate if the disaggregated dataset preserved characteristics important to flash flood prediction. An Extreme Value type I (EV1) distribution was fit to the maximum 30-minute intensity generated per calendar year, using the method of moments for the period 6/2000 - 12/2017. The ensemble mean frequency curve (from 100 ensemble members) was compared to the one generated from the filtered satellite data. Following verification, the single ensemble member which resulted in a 2000 - 2017 intensity-frequency curve closest to that from the GPM data was selected for further analysis.

Hydrologic Modeling Using SWAT

The Soil and Water Assessment Tool (SWAT) model (Arnold et al. 2013), used around the world for predicting streamflow in ungauged watersheds, was used to simulate flow in the *torrenteras*. SWAT is a comprehensive watershed model that evaluates impacts of land use, land management, and climate change on hydrology and water quality. Its sub-daily simulation option, critical for small watersheds like those of the *torrenteras* (Jeong et al. 2010; Boithias et al. 2017), was employed for this analysis. A radiometrically terrain corrected (RTC) elevation map with a 12.5 m resolution was obtained from the NASA Earth Data (NASA Earth Data 2019). An elevation-based watershed delineation process resulted in the creation of six watersheds (with drainage areas ranging from 5 to 36 km^2), and 79 sub-watersheds and streams (Figure 1). Watershed elevation ranged from 2258 to 5862 m along the steep side-slopes of Misti. Therefore, sub-watersheds were divided by elevation bands to consider orographic effects. Temperature data were taken from the SENAMHI and CORPAC stations and from gridded climate maps developed by Moraes et al. (2019) for the AltoMisti station. Precipitation and temperature of bands were adjusted based on the difference in elevation compared to the nearest weather station. Lapse rates (or change with altitude) of temperature (-6.2 °C/km) and precipitation (220 mm/km) were obtained from gridded climate maps developed by Moraes et al. (2019). Solar radiation, wind speed, and relative humidity simulations with 38 km resolution created by the National Center for Environmental Prediction (NCEP) Climate Forecast System Reanalysis (CFSR) were downloaded from the Global Weather Data for SWAT (NCEP CFSR 2019).

Soil and land cover properties were estimated from regional maps and soil profiles provided by the Peruvian Ministry of the Environment (Gobierno Regional Arequipa 2016; MINAM 2017) following the methodology developed by Daneshvar et al. (2020a; 2020b). Soil classes were defined based on taxonomy and suitability maps and soil properties were estimated for associated soil profiles. Land cover properties were adapted from similar land cover classes in the SWAT database. Plant growth properties were adjusted based on remotely sensed satellite Leaf Area Index time series and annual temperature maps for the region. Dominant land covers were grassland/shrub (42%), followed by cactus (21%), and urban lands (16%) (Table 1). Overlay of these layers resulted in 610 hydrologic response units (HRUs), which are the smallest subdivision of the SWAT model based on homogeneous combinations of land cover, soil, and slope in each subbasin.

There was no streamflow monitoring station within the watershed for model calibration and validation. Therefore, the same parameters from a neighboring watershed (Daneshvar et al. 2020c) were used. Daneshvar et al. (2020c) also showed that uncertainty of simulated streamflow based on the uncertainty of developed soil and land cover datasets (Daneshvar et al. 2020a; 2020b) is constrained (-7% to 10%) and the SWAT model provides reliable prediction of streamflow. SWAT simulations were conducted from February 1965 to December 2019. The first year of simulation was considered as model warm-up and was not included in further analysis. Model predictions of the 100-year flood for each *torrentera* were evaluated with respect to a regional curve (Moraes et al. 2020). The 54-year simulations (1966–2019) were used to calculate annual water balance ratios and several

Table 1. Watershed characteristics for the six *torrenteras* modeled in this study.

Torrentera	Watershed area (km^2)	Average slope (%)	------------- Land cover (%) -------------			
			Grassland/shrub	Cactus	Urban	Other*
Villa Ecológica	15.5	20.8	14	58	3	25
Polanco	15.2	24.4	72	15	7	6
Independencia	5.5	18.5	24	10	42	24
San Lázaro	18.5	40.2	46	15	11	28
Miraflores	14.9	18.8	18	21	42	19
Mariano Melgar	36.0	23.3	54	13	13	20

*Includes barren, herbaceous tundra, evergreen trees, and agricultural lands hydrologic metrics including the annual maxima series, the number of peak flow events over a threshold, time of rise during events, and number of days with flow (above 0.1 m^3/s). The SWAT-simulated 100-year floods were estimated by fitting an EV1 distribution to the annual maxima series of the daily average simulated streamflow. The annual maxima series was analyzed for monotonic trends using the non-parametric Mann-Kendall test, with significance level $p = 0.05$ (Helsel et al. 2020).

Local Data Collection

Undergraduate students at the Universidad Nacional de San Agustín de Arequipa took photos in all six *torrenteras* at the 26 bridge locations and at 29 channel sections in areas with no bridges. These photos were georeferenced, described, stored, and shared using Epicollect5, the free mobile data gathering platform. Channel locations visited were selected based on sections that were accessible and representative of that portion of the channel. A Phantom 4 Pro drone collected imagery of bridge locations that were difficult to access. Photos of channel sections were used to verify model inputs such as channel roughness, general channel shapes and bed material, as well as possible areas of concern for channel stability. Bridge and culvert dimensions, culvert roughness, and estimate contraction and expansion coefficients (see Figure 7B) were extracted from bridge photos. Bridge lengths were measured and used to scale other dimensions in the photos.

HEC-RAS Modeling

The Hydrological Engineering Center - River Analysis System (HEC-RAS) is used around the world for flood depth and hazard prediction (e.g., Stoleriu et al. 2019; Munir et al. 2020). A digital elevation model (DEM) with a horizontal resolution of 0.5 m and a vertical resolution of 1 m were imported as a terrain layer into RAS Mapper, part of HEC-RAS 5.0.7. *Torrenteras* are steep, straight channels dominated by one-dimensional (1D) flow. HEC-RAS 1D, which produced the best results for a flood study in a similar landscape (Bricker et al. 2017), was used to create hydraulic models for each to identify areas of hazard potential by assessing 1D variations in depth, velocity, and flood extent. Cross sections were placed at distances to account for changes in channel shape, slope, and at bridges and culverts. Bridge and culvert cross-sections were placed per guidelines in the HEC-RAS Hydraulic Reference Manual (USACE 2016). Expansion and contraction coefficients, culvert entrance losses, and ineffective flow areas were assigned according to the HEC-RAS Hydraulic Reference Manual (USACE 2016). Steady flow simulations of 100-year peak flow events in each *torrentera* were modeled using HEC-RAS 1D. Normal depth was used for boundary conditions, and upstream and downstream slopes were used as inputs.

Model parameters were adjusted so that maximum velocities did not exceed those recorded in similar channels (Magirl et al. 2009), because there was no data available for flood extent or water levels for calibration or validation at the time of this study. Channel roughness, or Manning's n, the parameter in HEC-RAS most sensitive to changes, was adjusted to meet this criterion (Ramesh et al. 2000; Parhi 2013). The same Manning's n, 0.12, was applied throughout all *torrenteras* because they had similar bed roughness, underlying geology, soil types, and sorting of heterogeneous sediments. This value is within the range of n values found in other steep sloped streams (Aguirre-Pe et al. 1990; Reid and Hickin 2008; Zimmerman 2010). Slopes in the modeled section of these *torrenteras* range from 0.04 - 0.10.

Flood Hazard Analysis

Analysis of Inundation Hazard. Water surface elevations modeled in HEC-RAS were imported to ArcMap 10.6 using the HEC-GeoRAS 10.6.0.1 plug-in for analysis and visualization. This mapping software was used to visualize inundation boundaries and identify infrastructure within the flood zone, like bridges, roads, and housing.

Analysis of Velocity Hazard. HEC-RAS model outputs for water velocity and depth in the torrenteras were used to characterize the potential for people and objects to be swept away, defined as the velocity hazard. In this paper, toppling was considered as the mechanism for loss of human stability, when the moment force caused by the floodwaters exceeds the moment force of the human body (Jonkman and Penning-Rowsell 2008). Literature thresholds are largely reported as empirical formulas determined from flume experiments to determine the point of loss of stability for humans (Jonkman and Penning-Rowsell 2008; Pisaturo et al. 2019) and vehicles (Martinez-Gomariz et al. 2016). For this paper, the velocity hazard was calculated as the product of water velocity and depth (Pisaturo et al. 2019), and an empirical equation (Karvonen et al. 2000) was used for the threshold of movement for a typical adult and child:

$$hv_c = 0.004Lm + 0.2 \quad (1)$$

where L is the height in meters, m is the mass in kg, and hv_c is the critical depth-velocity for instability. Using this equation, the instability threshold from toppling for a child 1.4 m tall and weighing 40 kg is 0.42 m^2/s, and the threshold for an adult (assuming the adult is 1.7 m tall and 70 kg) is 0.68 m^2/s. When the product of the model's flood velocity and depth is greater than this critical value, human stability is lost. When mapping velocity hazards from model results, thresholds were set as 0.4, 0.7, 2, and 8 m^2/s. These thresholds were set using Equation 1 for human stability and empirical literature values (Jonkman and Penning-Roswell 2008; Martiniz-Gomariz et al. 2016) and represent hazards capable of destabilizing a child (0.4 m^2/s), destabilizing adults and vehicles (0.7 m^2/s), complete loss of human stability (2 m^2/s), and separation between high and extremely high velocity hazards (8 m^2/s).

Analysis of Slope Instability Hazard. Slope failure occurs when the driving forces (conditional factors such as water and slope angle) are larger than resisting forces (intrinsic soil properties such as friction angle). The infinite slope method (Skempton and DeLory 1957) has been widely used as an estimate for slope stability under conditions with limited data. For this analysis, the soil was assumed to be cohesionless and dry, simplifying the factor of safety (FS) to Equation 2, where ϕ is the characteristic soil friction for a given soil and β is the angle of the slope.

$$FS = \frac{\tan(\phi)}{\tan(\beta)} \quad (2)$$

The soil was assumed to be silty sand (SM; United Soil Classification System; ASTM D2487-17el) based on classified soil data from nearby areas (MINAM 2017), and a value of 32.5 was used for ϕ (Prellwitz et al. 1994). For β, the 1 m *DEM* of the *torrenteras* was first smoothed using two-cell focal statistics, after which the percent slope was calculated. This allowed us to represent the critical slopes more accurately, particularly in areas with buildings. Factors of safety were then classified into stability classifications after Pisaturo et al. (2019). HEC-RAS outputs for stream power were also considered when determining areas with potential slope instability hazards. Stream power is used to express the flow energy of floodwaters and has been used to describe the potential for catastrophic geomorphic change (Magilligan et al. 2015).

Results

Hydrologic Analysis

Evaluation of Predictions. Thouret et al. (2014) provided a summary of 17 reported flood events that have occurred around Arequipa since 1915, with average precipitation intensities ranging from 4.5 to 73.5 mm/hr. They identified seven events with peak intensities greater than 30 mm/hr, implying a return period of about 14 years. The estimated intensity of 14-year return period events based on the disaggregated precipitation varied between 20 - 40 mm/hr. While it is not possible to directly compare these estimates, it seems that the generated frequencies are feasible based on limited recorded information of these extreme events in the area.

Figure 2 compares SWAT-predicted 100-year floods for the *torrenteras* with the regional regression developed from a Historic Reference Hydrologic Network (HRHN) (also shown) identified by Moraes et al. (2020). Estimated 100-year daily peak flows range from 213 m^3/s for Mariano Melgar to 32 m^3/s for Independencia. Given the strong association between all of these values, we conclude that the SWAT-simulated flood peak values provide a reasonable estimation of flood frequency for these ungauged basins.

Streamflow Characteristics. Analysis of 30-minute streamflow simulation over 54 years (1966 - 2019) showed that average annual flow ranged from 113 to 188 mm (37% to 46% of annual precipitation). Overall, these ephemeral streams are dry for almost

10 months per year on average and only flow 13% to 19% of the time.

As illustrated in Figure 3, streamflow events occur very rapidly in these steep channels, where peak flow is reached 30 - 60 minutes after the start of the event and total event duration is approximately 1 - 2 hours. In the 54-year SWAT simulations, maximum peak flow among all *torrenteras* occurred in Mariano Melgar, reaching 175 m^3/s, while San Lázaro peak flow exceeded 52 m^3/s. The flood of record varies among channels. The largest simulated peak in Independencia, San Lázaro, and Miraflores was in 2013, in response to the extreme 123 mm storm recorded at the La Pampilla station. This storm had very limited spatial extent, since very little precipitation was measured at the Rodríguez Ballón and Chiguata stations and did not cause substantial flooding in Villa Ecológica or Mariano Melgar. The flood of record for these two *torrenteras* occurred in 1976, while the flood of record in Polanco occurred in 1989.

Change Over Time. The daily precipitation record shows a statistically significant increase in the annual precipitation and the average daily depth of precipitation for the La Pampilla and Rodríguez Ballón stations. As a result, there has been an increase in the number of extreme precipitation events per year (Figure 4A).

This increase in extreme precipitation events translates into increasing frequency of peak flows (Figure 4B). All *torrenteras* exhibit an increasing tendency in the annual maxima series, but there is substantial spatial variability between locations. Based on the non-parametric Mann-Kendall test ($p = 0.05$), there is a statistically significant increasing trend in the simulated annual maxima series for Independencia, San Lázaro, and Mariano Melgar.

Flood frequency analysis was also performed for two time periods (1966 - 1990 and 1995 - 2020) to identify potential changes in the 100-year flood magnitude. The estimated 100-year flood magnitude has increased for the later period for the three channels for which 2013 was the flood of record, and it has decreased for the other three channels. As a result, only the 100-year floods estimated from the entire simulation period were used in the flood hazard assessment.

Hazard Mapping

In this section, we describe flood-related hazards associated with inundation, velocity, and slope

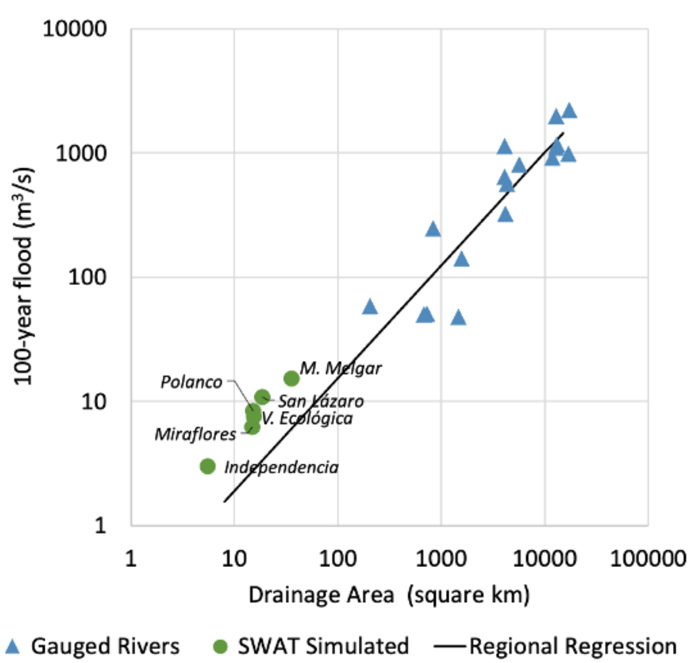

Figure 2. Log of the predicted 100-year discharge versus log drainage area for reference stream gauge locations in Arequipa (blue), estimated based on a regional regression developed from these gauges and the SWAT-simulated values for the *torrenteras*.

instability and provide case studies of problem areas for each hazard type.

Inundation Hazard. Peak flows from 100-year events showed that incidence and extent of flooding varied widely, but flood extents surpassed channel banks in at least one location in all modeled torrenteras. In all torrenteras, like the section of San Lázaro shown in Figure 5A, flooding was most likely in areas with large culvert constrictions. Overbank flow at non-bridge locations was less frequent but was often simulated in more densely urban areas where torrenteras

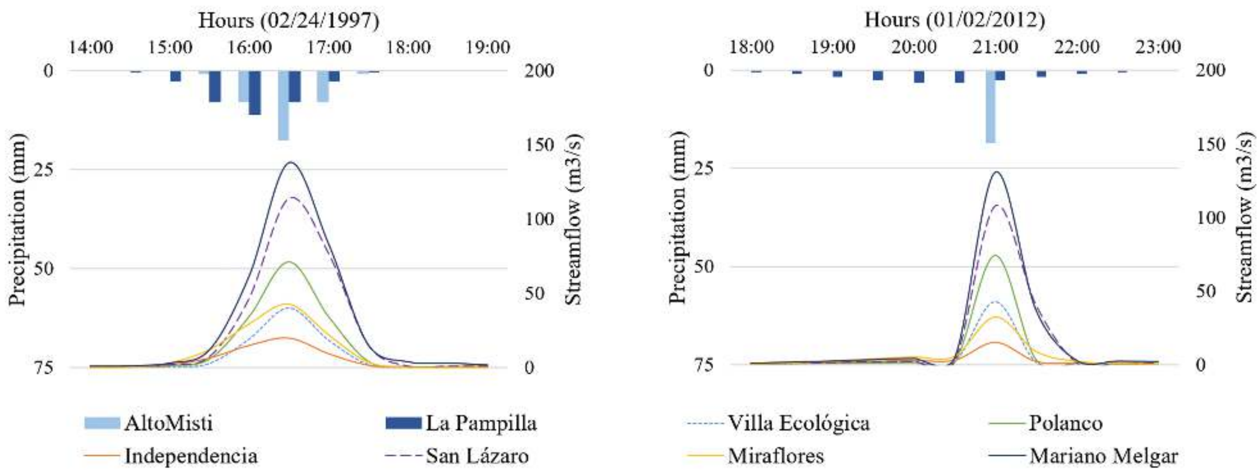

Figure 3. Simulated hydrographs for two flood events in six *torrenteras* and precipitation from the AltoMisti virtual station that was used as the precipitation station for the majority (65%) of the subbasins.

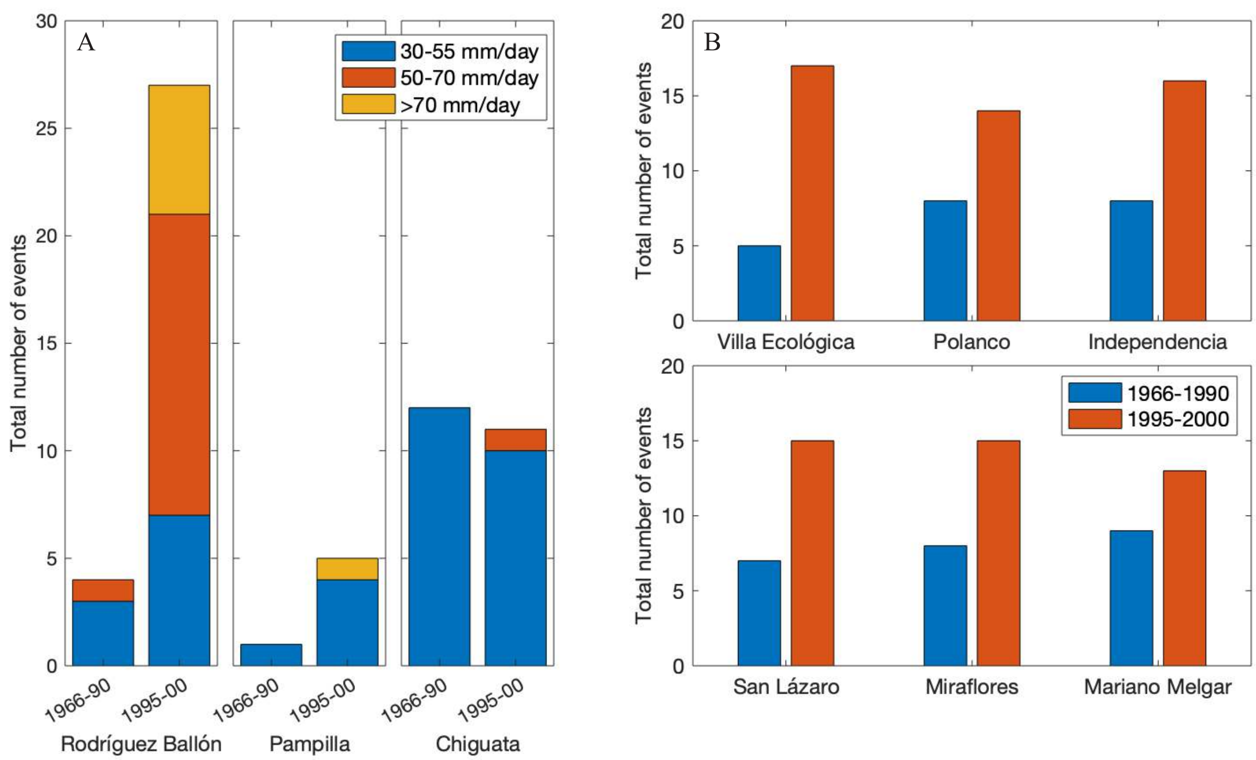

Figure 4. Hydrologic changes in Arequipa. A) Number of extreme precipitation events (> 30 mm/day) for the three weather stations closest to the *torrenteras.* B) Number of peaks over a threshold (two-year return period) in each of the six *torrenteras*.

were highly channelized, i.e., constricted within a constructed, concrete channel, like in Mariano Melgar (Figure 5B). In channelized areas with overbank flow, flooding was also simulated at bridges, which were even more constricted than the channels themselves. Flooding was of least concern in upstream areas where development did not encroach on the channel, the floodplain was accessible to floodwater, and bridge locations were wider and larger resulting in limited flow constriction. A good example for this is in the upstream area of San Lázaro (Figure 5C).

Velocity Hazard. Velocity hazard analysis for HEC-RAS outputs from the 100-year flow event are shown in Figure 6. Locations shown in Figure 6A, 6B, and 6C are the same as those shown in Figure 5A, 5B, and 5C, respectively. Most of the inundated area had high velocity hazard values that would cause an adult to topple over in the floodwater. Locations in Figure 6A and 6B are in the downstream, urbanized portion of the torrenteras and are heavily channelized with smaller flow areas. This led to greater velocities, deeper water, and therefore, increased velocity hazards compared to the upper portions of the torrenteras (Figure 6C). Location A also shows inundation of a road next to Mariano Melgar, where the velocity hazard exceeded thresholds for destabilizing adults and vehicles. Debris in floodwaters, like vehicles, also increases the velocity hazard and the likelihood of destabilizing other objects downstream (Jonkman and Penning-Rowsell 2008).

Slope Instability Hazard. Unstable slopes that could lead to failure occur when the slope FS is

Figure 5. Flood inundation extents of 100-year peak flows in A) Bridge Cahuide in San Lázaro, B) Bridge 8 de octubre and overland flow in Mariano Melgar, C) a less developed area upstream in San Lázaro with no overbank flow, and D) a location map for all aforementioned hazard sites.

less than 1.0. Figure 7 shows slope instability (as defined by the FS) and stream power in the upstream portion of San Lázaro (Figure 6C), as well as drone imagery of the bridge in this section of the torrentera. Since stream power indicates the work a stream is capable of doing, such as sediment transport, areas with high stream power and high slope instability are areas with high slope failure potential. In the middle portion of Figure 7A (location 1), slopes surrounding the channel are unstable and the stream power is high. Areas like this of high instability and high stream power are most susceptible to slope failure. In the upper portion (location 2) of Figure 7A, San Lázaro is wider and the floodwater has more area in which to disperse, lowering the stream power. This area could have a lower slope instability hazard than location 1 because, although the slopes are still steep and unstable, the floodwater has less power to destabilize the sediment. Immediately above the bridge (location 3), the slope instability and stream power are lower, meaning this area would have a lower slope instability hazard.

Discussion

Applications of Flood Hazard Information

Though estimated 100-year peak flows have not increased over the period of study in all *torrenteras*, our analysis demonstrated that moderate flood events are becoming more frequent. Hydrologic analysis shows that stormflow is unpredictable, flashy, and can be very isolated. These flows, though infrequent, happen very quickly, reaching peak flow in an hour or less. Arequipa is growing, and urban development near and into the *torrenteras* is increasing (Figure 8A). Hazard maps show that many areas in and around the *torrenteras*

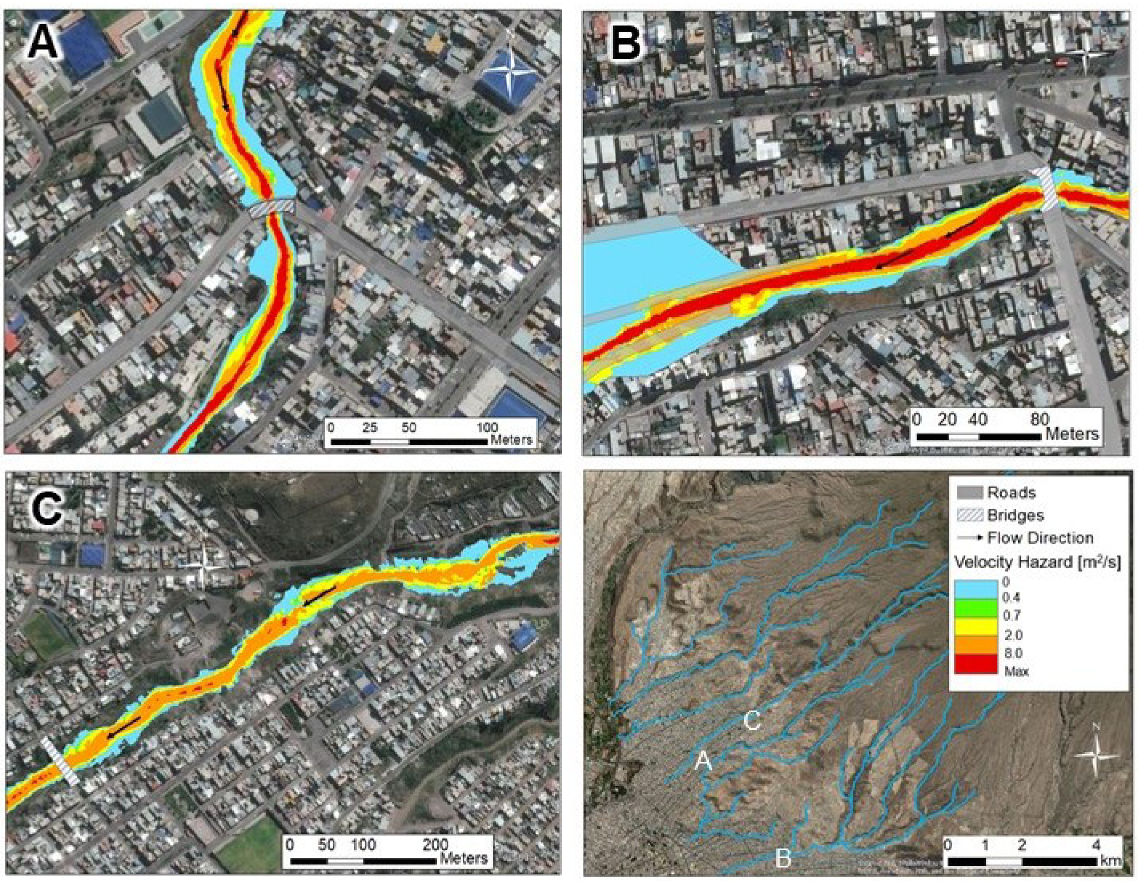

Figure 6. Velocity hazard maps for the case studies using HEC-RAS outputs from the 100-year peak flow for water velocity and depth at A) Bridge Cahuide in San Lázaro, B) Bridge 8 de octubre and overland flow in Mariano Melgar, C) a less developed area upstream in San Lázaro, and D) a location map for all aforementioned hazard sites.

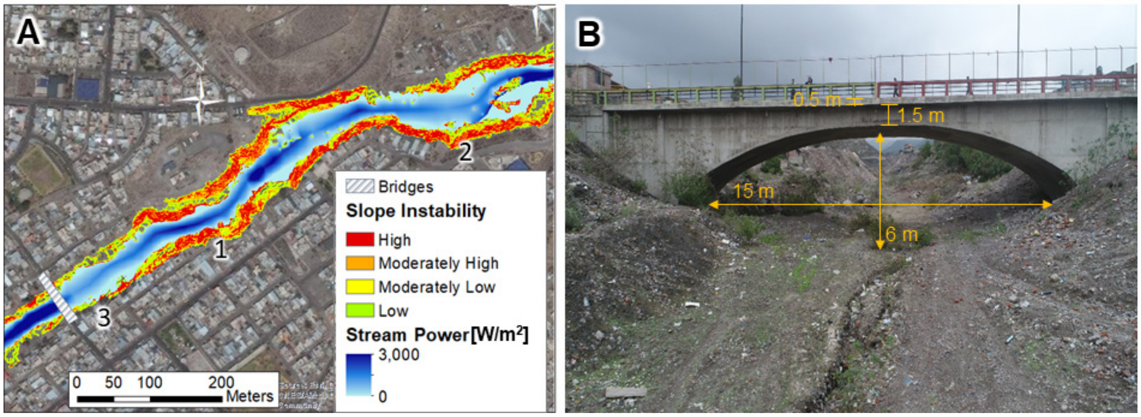

Figure 7. A) Slope instability and stream power of San Lázaro at three selected locations (1, 2, and 3). B) Drone footage of the bridge over San Lázaro depicted in A (location 3) and how it was used to get bridge dimensions. Slope instability is considered high when FS is less than 1, moderately high when FS is between 1 and 1.25, moderately low when FS is between 1.25 and 1.5, and low when FS is greater than 1.5.

can be dangerous, but these issues are exacerbated as development encroaches on the channels, putting more people and property at risk from flood hazards (Figure 8B). Hydraulic modeling and analysis of inundation, velocity, and slope instability give examples of hazards during the most extreme events, which can provide guidance for dealing with other, less severe floods. It is becoming increasingly important that stakeholder groups utilize hazard mapping information to make decisions about disaster mitigation strategies and future development. We provide considerations for each stakeholder group based on hazard locations, such as those shown in Figure 8B for a section of Mariano Melgar.

Use by Stakeholders

Reliable hazard maps could enhance flash flood mitigation strategies already in place in Arequipa. Currently, a rudimentary early warning system exists, relying on those living in upstream areas to report landslides and floods (Andina 2013). There are plans to add advanced weather prediction to the warning system, making it more robust and allowing for more time to evacuate (Del Mar 2019). Different mitigation strategies have been used in flash flood-prone areas to increase channel stability. Concrete reinforcement has been used in *torrenteras* to increase stability based on site observation. Colombo et al. (2002) created an extensive list of structures that have been effective in managing flash floods throughout Europe, including the use of gabion walls and natural materials for bank erosion protection. Land use control, like leaving vulnerable floodplains undeveloped or converting them into flood tolerable green spaces, has been utilized to mitigate flood damage in arid regions around the world (Abdrabo et al. 2020).

Information on flood boundaries where streamflow leaves the channel can help disaster risk managers and emergency responders make decisions about which bridges to close first, areas to prioritize for evacuation because of higher hazard probabilities, and optimal routes for evacuation. Velocity hazards can be used to issue warnings of areas to avoid during storm events because the storm duration and rapidly rising waters characteristic of flash floods give emergency responders little time to prepare and respond to extreme events. Lastly, areas where banks of the *torrenteras* have the highest slope instability hazards can be monitored more closely during storm events when soil saturation increases the probability of failure.

Water authorities can use this information about high hazard zones to establish limits for flood boundaries and, therefore, development, in currently less-developed, upstream areas. These boundaries can be based on identified floodplains and unstable slopes, minimizing hazards caused by channelization and floodplain encroachment. Although these regulations may be difficult to enforce as informal settlements encroach on *torrentera* channels, this study, with both hydrologic and hydraulic analysis of peak flows in *torrenteras,* provides scientific guidance on where and how to set development limits.

Though it is difficult to alter existing infrastructure in developed areas without large investment and displacement of people, municipalities and planners can prioritize areas in which to work with vulnerable people to utilize measures at the home-scale to mitigate flood risk, which can be much more cost-effective (Holub and Fuchs 2008).

While hazard mapping provides planners with limits for regulating development, for these *torrenteras*, there is no guarantee that community groups will not create "informal settlements" in high hazard zones. To increase the likelihood of community acceptance, community education of these hazards and consequences of floodplain encroachment is key (Zeballos-Velarde et al. 2017). In addition, upstream areas with more open and available space could be used to mitigate flooding effects farther downstream. Streamflow can be slowed or diverted to reduce downstream impact, through methods like creating check dams and step pools (Norman et al. 2016), offline detention (Ngo et al. 2016), and diverting water to spreading grounds that allow for sedimentation and infiltration (Wohlgemuth and Lilley 2018). Costs

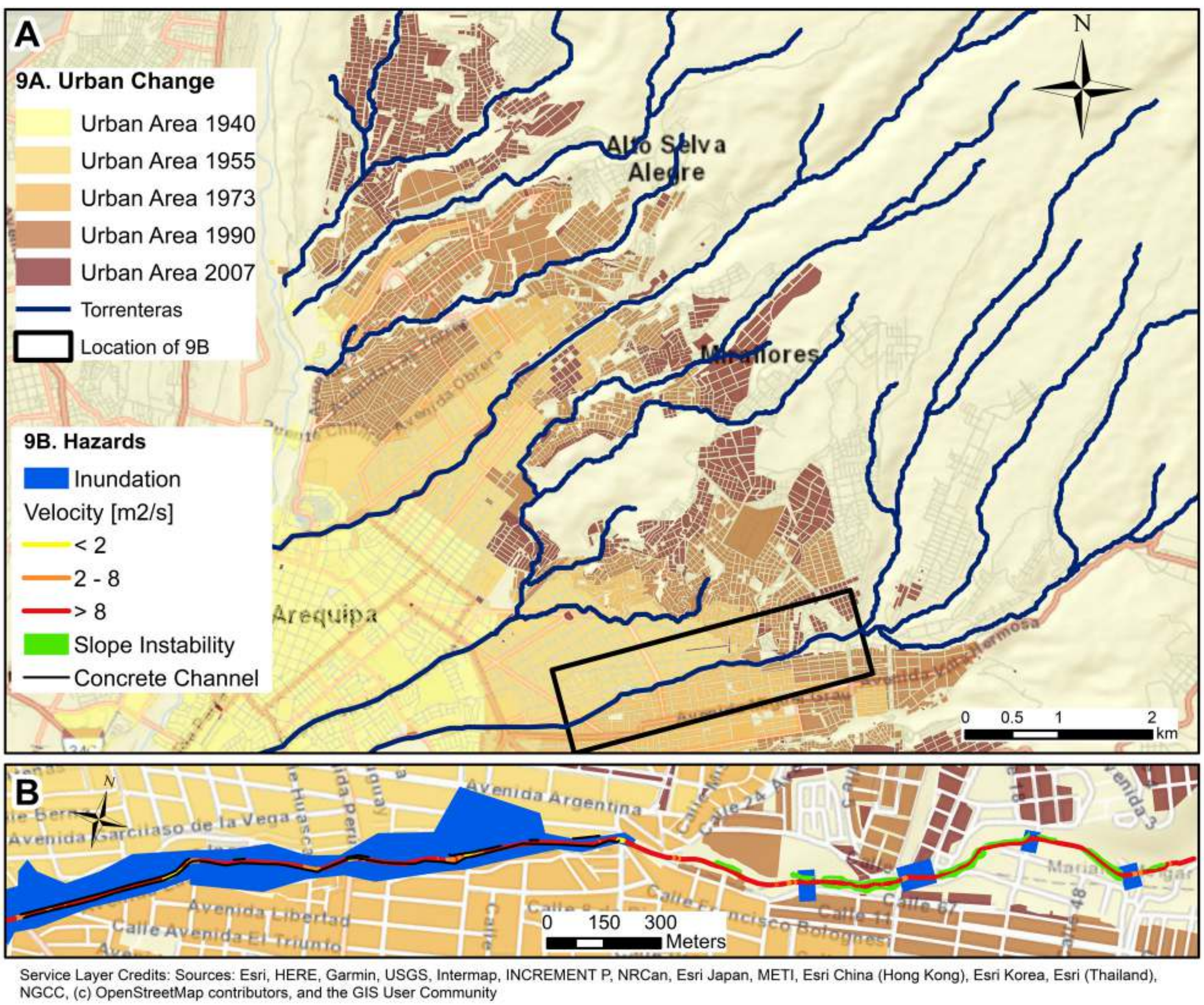

Figure 8. A) Development of Arequipa over time near the *torrenteras* indicates the importance of understanding flood hazards. B) Identified hazards have been compiled in a section of Mariano Melgar, showing areas of highest concern. These areas identify zones of flood hazard rather than exact flood extent.

of maintenance, like removal of heavy sediment loads, should be considered when implementing any of these options (Aerts 2018). With decreased velocity hazard and because they only convey water two months per year, there may be opportunities to use *torrenteras* for recreational infrastructure as a community amenity (Remón Royo 2018). The *torrenteras,* like other ephemeral streams, may also be enhanced to provide ecosystem services, including cultural services for nearby communities (Koundouri et al. 2017; Datry et al. 2018).

Conclusions

Intense peak flows, combined with channelization and development near or into the *torrenteras* of Arequipa, cause hazards for both human life and infrastructure. The city's ability to mitigate damage from these events has been limited due to a lack of both meteorological and topographical information. In this study, we had access to high-resolution spatial data and were able to synthesize sub-daily precipitation using a combination of datasets, which allowed us to assess hydrologic and hydraulic impacts from storm events over the last 60 years in the *torrenteras*. Storms are short and intense, resulting in high peak flows and short time to peak. The intensity of precipitation is increasing in some parts of the city, and the frequency of moderate flood peaks is increasing.

Hydraulic analysis revealed flood hazards related to inundation, velocity, and slope instability. Flooding was an issue in all modeled channels, particularly at bridges and culverts in downstream, channelized sections of the *torrenteras*. When channelization was very extreme, like in areas where development abutted concrete-reinforced channels, there was even inundation on roads and around houses. All *torrenteras* had large stretches where the velocity hazards were large enough to destabilize both humans and vehicles, and these flows become more extreme in channelized sections of the *torrenteras*. Development has also moved into unstable channel sections, encroaching on the channel floodplain, and putting these buildings in danger of collapse.

This analysis of hazards can be used for multiple stakeholder groups in Arequipa. This method can be used to create extensive, detailed maps for all *torrenteras*, thus providing these groups with specific information on hazard areas. Using this information, disaster risk managers can create evacuation routes, prioritize road closures, and create warnings of high hazard zones. Water authorities, municipalities, and planners can work together to create development boundaries based on hazard maps. Planners can also engage with community members to build understanding of where hazards exist in the *torrenteras* and the importance of respecting development boundaries.

Acknowledgments

Funds to support research in the Arequipa Nexus Institute for Food, Energy, Water, and the Environment were provided by the Universidad Nacional de San Agustín. The DEM was provided by the "Costuras Urbanas: Red de Centralidades Barriales en la Periferia de Arequipa como alternativa Socio Ambiental al Cambio Climático en Poblaciones Vulnerables" research project, funded by the Universidad Nacional de San Agustín.

Author Bio and Contact Information

Katy Mazer (corresponding author) is coordinator of the Sustainable Water Management team of The Nexus Institute at Purdue University. She engages with stakeholder groups in Arequipa, Peru to coproduce water management decision-making tools. She can be contacted at kmazer@purdue.edu or 920 W. State St., West Lafayette, IN 47907.

Abigail Tomasek is a Postdoctoral Research Associate in Agricultural and Biological Engineering at Purdue University. Her research broadly focuses on how anthropogenic activities have affected water quality and flow using a combination of experimental and field-based methods. She can be contacted at atomasek@purdue.edu.

Fariborz Daneshvar is a Postdoctoral Research Associate in the Department of Agricultural and Biological Engineering at Purdue University. He conducts watershed hydrology research with respect to environmental and socioeconomic impacts. He can be contacted at fdaneshv@purdue.edu or 225 S. University St., West Lafayette, IN 47907.

Laura Bowling is a Professor of hydrology in the Department of Agronomy at Purdue University. Her research investigates the water resources impact of environmental change across multiple scales, climate

regimes, and ecosystems and communicates these findings to stakeholders. She can be contacted at bowling@purdue.edu or 915 W. State St., West Lafayette, IN 47907.

Jane Frankenberger is a Professor of Agricultural and Biological Engineering at Purdue University. She conducts model-based analyses and engages stakeholders to improve management of watersheds and water quality. She can be contacted at frankenb@purdue.edu or 225 S. University St., West Lafayette, IN 47907.

Sara McMillan is an Associate Professor of Agricultural and Biological Engineering at Purdue University. Her research on ecological restoration uses experimental and modeling approaches to develop solutions to water quality problems. She can be contacted at smcmillan@purdue.edu or 225 S. University St. West Lafayette, IN 47907.

Hector Novoa is a professor of fluid mechanics, hydraulics and hydrology in the Faculty of Civil Engineering at the Universidad Nacional de San Agustín in Arequipa, Peru. He has over 25 years of experience in environmental issues, including water and sewer systems, surface water hydrology, and design of hydraulic structures. He can be contacted at hnovoa@unsa.edu.pe.

Carlos Zeballos-Velarde is an architect, urban planner, and professor in the Faculty of Architecture and Urbanism at the Universidad Nacional de San Agustín in Arequipa, Peru. He conducts GIS analyses about various topics related to environmental urban planning and works on several research projects about participatory risk management with different communities. He can be contacted at czeballos@unsa.edu.pe or Urb. Las Begonias F-1, JLByR. Arequipa, Peru.

References

Abdrabo, K.I., S.A. Kantosh, M. Saber, T. Sumi, O.M. Habiba, and B. Alboshy. 2020. The Role of Urban Planning Tools in Flash Flood Risk Reduction for The Urban Arid and Semi-Arid Regions. DOI:10.13140/RG.2.2.31397.12000.

Aerts, J.C.J.H. 2018. A review of cost estimates for flood adaptation. *Water* 10(11): 1646. Available at: https://doi.org/10.3390/w10111646. Accessed November 24, 2020.

Aguirre-Pe, J. and R. Fuentes. 1990. Resistance to flow in steep rough streams. *Journal of Hydraulic Engineering* 116(11): 1374-1387. Available at: https://doi.org/10.1061/(ASCE)0733-9429(1990)116:11(1374). Accessed March 19, 2020.

Andina. 2013. Instalan sistema de alerta temprana en Arequipa para prevenir desastres por lluvias. Agencia Peruana de Noticias. Available at: https://andina.pe/agencia/noticia.aspx?id=487435. Accessed November 23, 2020.

Arnold, J.G., J.R. Kiniry, R. Srinivasan, J.R. Williams, E.B. Haney, and S.L. Neitsch. 2013. Soil & Water Assessment Tool. Input/Output Documentation Version 2012. Texas Water Resources Institute, TR-439. Available at: https://swat.tamu.edu/media/69296/swat-io-documentation-2012.pdf. Accessed April 30, 2020.

ASTM D2487-17e1. 2017. Standard Practice for Classification of Soils for Engineering Purposes (United Soil Classification System). ASTM International, West Conshohocken, PA. Available at: https://www.astm.org/Standards/D2487.htm. Accessed May 1, 2020.

Boithias, L., S. Sauvage, A. Lenica, H. Roux, K.C. Abbaspour, K. Larnier, D. Dartus, and J.M. Sánchez-Pérez. 2017. Simulating flash floods at hourly time-step using the SWAT model. *Water* 9(12): 929. Available at: https://doi.org/10.3390/w9120929. Accessed March 13, 2020.

Bowling, L.C., D.P. Lettenmaier, B. Nijssen, L.P. Graham, D.B. Clark, M. El Maayar, R. Essery, S. Goers, Y.M. Gusev, F. Habets, B. van den Hurk, J. Jin, D. Kahan, D. Lohmann, X. Ma, S. Mahanama, D. Mocko, O. Nasonova, G.Y. Niu, P. Samuelsson, A.B. Shmakin, K. Takata, D. Verseghy, P. Viterbo, Y. Xia, Y. Xue, and Z.L. Yang. 2003. Simulation of high-latitude hydrological processes in the Torne-Kalix basin: PILPS Phase 2(e) 1: Experiment description and summary intercomparisons. *Journal of Global and Planetary Change* 38(1-2): 1-30. Available at: https://doi.org/10.1016/S0921-8181(03)00003-1. Accessed March 13, 2020.

Bricker, J.D., W. Schwanghart, B.R. Adhikari, S. Moriguchi, V. Roeber, and S. Giri. 2017. Performance of models for flash flood warning and hazard assessment: The 2015 Kali Gandaki landslide dam breach in Nepal. *Mountain Research and Development* 37(1): 5-15. Available at: https://doi.org/10.1659/MRD-JOURNAL-D-16-00043.1. Accessed November 30, 2020.

Cacya, L., P. Meza, V. Carlotto, and L. Mamani. 2013. Aluvión del 8 de Febrero del 2013 en la ciudad de Arequipa. In: *Foro Internacional Peligros Geológicos,* INGEMMET, Arequipa, Peru, pp. 195-200. Available at: https://hdl.handle.net/20.500.12544/1132. Accessed November 30, 2020.

Colombo, A.G., J. Hervas, and A.L. Vetere Arellano. 2002. *Guidelines on Flash Flood Prevention and Mitigation*. European Commission Joint Research Centre, Report number EU-NA-20-386-EN-C. Available at: https://www.researchgate.net/deref/http%3A%2F%2Fdx.doi.org%2F10.13140%2FRG.2.1.4234.2480. Accessed December 2, 2020.

Daneshvar, F., J.R. Frankenberger, L.C. Bowling, K.A. Cherkauer, and M.J. Villalta Soto. 2020a. Estimated Soil Physical Properties for Hydrologic Modeling in Arequipa, Peru. Purdue University Research Repository. DOI: 10.4231/N5MX-9W30.

Daneshvar, F., J.R. Frankenberger, L.C. Bowling, K.A. Cherkauer, and J.A. Vera Mercado. 2020b. Estimated Land Cover Properties for Hydrologic Modeling in Arequipa, Peru. Purdue University Research Repository. DOI: 10.4231/GYN8-W684.

Daneshvar, F., J.R. Frankenberger, L.C. Bowling, K.A. Cherkauer, and A.G.D.L. Moraes. 2020c. Development of strategy for SWAT hydrologic modeling in data-scarce regions of Peru. *Journal of Hydrologic Engineering* (Under Review).

Datry, T., A.J. Boulton, N. Bonada, K. Fritz, C. Leigh, E. Sauguet, K. Tockner, B. Hugueny, and C.N. Dahm. 2018. Flow intermittence and ecosystem services in rivers of the Anthropocene. *Journal of Applied Ecology* 55(1): 353-364. Available at: https://doi.org/10.1111/1365-2664.12941. Accessed April 17, 2020.

Del Mar, J. 2019. Arequipa: El radar de 3 millones de soles que financiaría Cerro Verde permitirá pronosticar lluvias. *El Búho*. Available at: https://elbuho.pe/2019/03/arequipa-radar-metereologico-senamhi-lluvias-cerro-verde/. Accessed November 23, 2020.

Gobierno Regional Arequipa. 2016. Elaboración del Estudio de Suelos y la Clasificación de Tierras por su Capacidad de Uso Mayor en la Región Arequipa. Proyecto Desarrollo de Capacidades en Zonificación Ecológica Económica para el Ordenamiento Territorial en la Región Arequipa, Autoridad Regional Ambiental de Arequipa, Gobierno Regional Arequipa, Arequipa, Perú. 1,152 pp. (Reg.# 1782331, Doc.# 1775929).

Gourley, J.J., Z.L. Flamig, H. Vergara, P.E. Kirstetter, R.A. Clark III, E. Argyle, A. Arthur, S. Martinaitis, G. Terti, J.M. Erlingis, and Y. Hong. 2017. The FLASH project: Improving the tools for flash flood monitoring and prediction across the United States. *Bulletin of the American Meteorological Society* 98(2): 361-372. DOI:10.1175/BAMS-D-15-00247.1.

He, B., X. Huang, M. Ma, Q. Chang, Y. Tu, Q. Li, K. Zhang, and Y. Hong. 2018. Analysis of flash flood disaster characteristics in China from 2011 to 2015. *Natural Hazards* 90(3): 407-420. DOI:10.1007/s11069-017-3052-7.

Helsel, D.R., R.M. Hirsch, K.R. Ryberg, S.A. Archfield, and E.J. Gilroy. 2020. Statistical methods in water resources. In: *U.S. Geological Survey Techniques and Methods, book 4, chapter A3*, Reston, VA. Available at: https://doi.org/10.3133/tm4a3. Accessed November 30, 2020.

Holub, M. and S. Fuchs. 2008. Benefits of local structural protection to mitigate torrent-related hazards. In: *Risk Analysis VI: Simulation and Hazard Mitigation*, C.A. Brebbia and E. Beriatos (Eds.). WIT Press, Southampton, UK, pp. 401-411.

Huffman, G., D. Bolvin, D. Braithwaite, K. Hsu, R. Joyce, and P. Xie. 2019. Integrated Multi-satellite Retrievals for GPM (IMERG), version 6. NASA's Precipitation Processing Center. Available at: https://giovanni.gsfc.nasa.gov/giovanni/. Accessed October 31, 2019.

Jeong, J., N. Kannan, J. Arnold, R. Glick, L. Gosselink, and R. Srinivasan. 2010. Development and integration of sub-hourly rainfall–runoff modeling capability within a watershed model. *Water Resources Management* 24(15): 4505-4527. Available at: https://doi.org/10.1007/s11269-010-9670-4. Accessed March 13, 2020.

Jonkman, S.N. and E. Penning-Rowsell. 2008. Human instability in flood flows. *Journal of the American Water Resources Association* 44(5): 1208-1218. Available at: https://doi.org/10.1111/j.1752-1688.2008.00217.x. Accessed March 15, 2020.

Karvonen, R.A., A. Hepojoki, H.K. Huhta, and A. Louhio. 2000. *The Use of Physical Models in Dam-break Analysis*. RESCDAM Final Report of Helsinki University of Technology, Helsinki, Finland. Available at: https://www.google.com/search?q=The+use+of+physical+models+in+dam-break+analysis%2C+RESCDAM+Final+Report%2C+Helsinki+University+of+Technology&rlz=1C1CHBF_enUS798US798&oq=The+use+of+physical+models+in+dam-break+analysis%2C+RESCDAM+Final+Report%2C+Helsinki+University+of+Technology&aqs=chrome..69i57j69i64.318j0j7&sourceid=chrome&ie=UTF-8#. Accessed December 2, 2020.

Koundouri, P., A.J. Boulton, T. Datry, and I. Souliotis. 2017. Ecosystem services, values, and societal perceptions of intermittent rivers and ephemeral streams. In: *Intermittent Rivers and Ephemeral Streams*, Academic Press, pp. 455-476. Available at: https://doi.org/10.1016/B978-0-12-803835-2.00018-8. Accessed April 17, 2020.

Magilligan, F.J., E.M. Buraas, and C.E. Renshaw. 2015. The efficacy of stream power and flow duration on geomorphic responses to catastrophic flooding. *Geomorphology* 228: 175-188. Available at: https://doi.org/10.1016/j.geomorph.2014.08.016. Accessed March 15, 2020.

Magirl, C.S., J.W. Gartner, G.M. Smart, and R.H. Webb. 2009. Water velocity and the nature of critical flow in large rapids on the Colorado River, Utah. *Water Resources Research* 45(5): W05427. Available at: https://doi.org/10.1029/2009WR007731. Accessed March 19, 2020.

Martelli, K.M. 2011. The physical vulnerability of urban areas facing the threat of inundation from lahars and floods: Application to the city of Arequipa, Peru. Dissertation, Université Blaise Pascal, Clermont-Ferrand, France. Available at: https://tel.archives-ouvertes.fr/tel-00881754/. Accessed November 16, 2019.

Martinez-Gomariz, E., M. Gomez Valentin, B. Russo, and S. Djordjevic. 2016. Stability criteria for flooded vehicles: A state of the art review. *Flood Risk Management* 11(1). Available at: https://doi.org/10.1111/jfr3.12262. Accessed March 15, 2020.

Ministerio de Ambiente (MINAM). 2017. Zonificación Ecológica y Económica (ZEE). Available at: https://www.minam.gob.pe/ordenamientoterritorial/zonificacion-ecologica-y-economica-zee/. Accessed November 26, 2019.

Moraes, A.G., K.A. Cherkauer, L.C. Bowling, and C.R. Zeballos Velarde. 2019. Arequipa Climate Maps-Normals. Purdue University Research Repository. DOI: 10.4231/490D-HC66.

Moraes, A.G.L., E. Bocardo-Delgado, L. Bowling, F. Daneshvar, J. Pinto, A.H. Watkins, and K.A. Cherkauer. Assessment of Arequipa's Hydrometeorological Monitoring Infrastructure to Support Water Management Decisions. *Journal of Contemporary Water Research and Education* 171: 27-48. Available at: https://onlinelibrary.wiley.com/journal/1936704x. Accessed December 22, 2020.

Muller, M. 2007. Adapting to climate change: Water management for urban resilience. *Environment and Urbanization* 19(1): 99-113. Available at: https://doi.org/10.1177%2F0956247807076726. Accessed November 16, 2020.

Munir, B.A., S.R. Ahmad, and S. Hafeez. 2020. Integrated hazard modeling for simulating torrential stream response to flash flood events. *ISPRS International Journal of Geo-Information* 9(1): 1. Available at: https://doi.org/10.3390/ijgi9010001. Accessed December 2, 2020.

NASA Earth Data. 2019. ASF Data Search Vertex. Available at: https://search.asf.alaska.edu/#/?flightDirs=. Accessed October 10, 2019.

The National Centers for Environmental Prediction, Climate Forecast System Reanalysis (NCEP CFSR). 2019. Global Weather Data for SWAT. Available at: https://globalweather.tamu.edu. Accessed October 29, 2019.

Ngo, T.T., D.G. Yoo, Y.S. Lee, and J.H. Kim. 2016. Optimization of upstream detention reservoir facilities for downstream flood mitigation in urban areas. *Water* 8(7): 290. Available at: https://doi.org/10.3390/w8070290. Accessed April 17, 2020.

Norman, L.M., F. Brinkerhoff, E. Gwilliam, D.P. Guertin, J. Callegary, D.C. Goodrich, P.L. Nagler, and F. Gray. 2016. Hydrologic response of streams restored with check dams in the Chiricahua Mountains, Arizona. *River Research and Applications* 32(4): 519-527. Available at: https://doi.org/10.1002/rra.2895. Accessed April 29, 2020.

Parhi, P.K. 2013. HEC-RAS model for Manning's roughness: A case study. *Open Journal of Modern Hydrology* 3: 97-101. Available at: http://www.scirp.org/journal/ojmh. Accessed March 19, 2020.

Pisaturo, G.R., M. Righetti, C. Castellana, M. Larcher, A. Menapace, and G. Premstaller. 2019. A procedure for human safety assessment during hydropeaking events. *Science of the Total Environment* 661: 294-305. Available at: https://doi.org/10.1016/j.scitotenv.2019.01.158. Accessed December 2, 2020.

Prellwitz, R., T. Koler, and J. Steward. 1994. *Slope Stability Reference Guide for National Forests in the United States – Volume II*. Engineering Management Report EM-1710-13, U.S. Department of Agriculture, Forest Service, Washington, D.C. Available at: https://www.google.com/books/edition/_/KpFedYt9r7oC?gbpv=1. Accessed December 2, 2020.

Ramesh, R., B. Datta, S.M. Bhallamudi, and A. Narayana. 2000. Optimal estimation of roughness in open-channel flows. *Journal of Hydraulic Engineering* 126(4): 299-303. Available at: https://doi.org/10.1061/(ASCE)0733-9429(2000)126:4(299). Accessed March 19, 2020.

Reid, D.E. and E.J. Hickin. 2008. Flow resistance in steep mountain streams. *Earth Surface Processes and Landforms* 33(14): 2211-2240. Available at: https://doi.org/10.1002/esp.1682. Accessed March 19, 2020.

Remón Royo, R. 2018. Basureros transformados en jardines públicos: Medellín, Colombia. *Arquitectura y Empresa*. Available at: https://www.arquitecturayempresa.es/

noticia/basureros-transformados-en-jardines-publicos-medellin-colombia. Accessed April 26, 2020.

Republica de Perú. 2016. Reglamento para la Delimitación y Mantenimiento de Fajas Marginales. Resolución Jefatural No 332-2016-ANA. Available at: http://www.osterlingfirm.com/Documentos/webma/normas/RJ-332-2016-ANA.pdf. Accessed December 2, 2020.

Rodriguez-Iturbe, I., D.R. Cox, and V. Isham, 1987. Some models for rainfall based on stochastic point processes. *Proceedings of the Royal Society of London. Series A, Mathematical and Physical Sciences* 410(1839): 269-288. Available at: https://doi.org/10.1098/rspa.1987.0039. Accessed December 2, 2020.

Servicio Nacional de Meteorología e Hidrología del Perú (SENAMHI). 2019. Ministerio del Ambiente. Available at: https://www.senamhi.gob.pe/. Accessed October 29, 2019.

Sistema Nacional de Defensa Civil Peru (SINPAD). 2013. Fuertes Precipitaciones Pluviales Afectaron la Ciudad de Arequipa. Estado Situacional de la Emergencia. Available at: http://sinpad.indeci.gob.pe/sinpad/emergencias/Evaluacion/Reporte/rpt_eme_situacion_emergencia.asp?EmergCode=00056271. Accessed April 30, 2020.

Skempton, A.W. and F.A. DeLory. 1957. Stability of natural slopes in London clay. In: *Proceedings of the 4th International Conference on Soil Mechanics and Foundation Engineering 2*, Thomas Telford Publishing, London, England, pp. 378-381. Available at: https://doi.org/10.1680/sposm.02050.0011. Accessed December 2, 2020.

Stoleriu, C.C., A. Urzica, and A. Mihu-Pintilie. 2019. Improving flood risk map accuracy using high-density LiDAR data and the HEC-RAS river analysis system: A case study from north-eastern Romania. *Journal of Flood Risk Management* 13(3): e12572. Available at: https://www.researchgate.net/deref/http%3A%2F%2Fdx.doi.org%2F10.1111%2Fjfr3.12572. Accessed December 2, 2020.

Teutschbein, C. and J. Seibert, 2012. Bias correction of regional climate model simulations for hydrological climate-change impact studies: Review and evaluation of different methods. *Journal of Hydrology* 456-457: 12-29. Available at: https://doi.org/10.1016/j.jhydrol.2012.05.052. Accessed December 2, 2020.

Thouret, J.-C., S. Ettinger, M. Guitton, O. Santori, C. Magill, K. Martelli, G. Zuccaro, V. Revilla, J.A. Charca, and A. Arguedas. 2014. Assessing physical vulnerability in large cities exposed to flash floods and debris flows: The case of Arequipa (Peru). *Natural Hazards* 73: 1771-1815. Available at: https://doi.org/10.1007/s11069-014-1172-x. Accessed November 16, 2019.

Thouret, J.-C., G. Enjolras, K. Martelli, O. Santoni, A. Luque, M. Nagata, A. Arguedas, and L. Macedo. 2013. Combining criteria for delineating lahar- and flash-flood-prone hazard and risk zones for the city of Arequipa, Peru. *Natural Hazards and Earth Systems Science* 13: 339-360. DOI: 10.5194/nhess-13-339-2013.

U.S. Army Corps of Engineers (USACE). 2016. HEC-RAS River Analysis System. Hydraulic Reference Manual, Version 5.0, CPD-69. U.S. Army Corps of Engineers Hydraulic Engineering Center, Davis, California. Available at: https://www.hec.usace.army.mil/software/hec-ras/documentation/HEC-RAS%205.0%20Reference%20Manual.pdf. Accessed December 2, 2020.

Wohlgemuth, P.M. and K.A. Lilley. 2018. Sediment delivery, flood control, and physical ecosystem services in southern California Chaparral Landscapes. In: *Valuing Chaparral*, E. Underwood, H. Safford, N. Molinari, and J. Keeley (Eds.). Springer, Cham, pp. 181-205. Available at: https://doi.org/10.1007/978-3-319-68303-4_7. Accessed November 17, 2020.

Zeballos-Velarde, C., M.Á. Huamaní, J.Q. Valdivia, S.C. Alejo, and C.M. Espinoza. 2019. An environmental atlas as a tool for improving local environmental education and awareness in Arequipa. In: *Proceedings of the International Congress on Educational and Technology in Sciences*, Arequipa, Peru, December 10-12, 2019, pp. 191-200. Available at: http://ceur-ws.org/Vol-2555/paper17.pdf. Accessed April 13, 2020.

Zeballos-Velarde, C., R. Gonzalez-Salinas, and J. Urquizo Angulo. 2017. Urban linkages: A methodological framework for a network neighbour centralities in the periphery of Arequipa, Peru, as a social-environmental alternative to climate change in vulnerable settlements. In: *Proceedings of the UIA 2017 Seoul World Architects Congress*, September 3-7, 2017, Seoul, Korea. Available at: http://www.uia2017seoul.org/P/assets/html/5-2-paper.html. Accessed December 2, 2020.

Zimmerman, A. 2010. Flow resistance in steep streams: An experimental study. *Water Resources Research* 46(9): W09536. Available at: https://doi.org/10.1029/2009WR007913. Accessed March 19, 2020.